American Journal of Engineering Research (AJER)
e-ISSN: 2320-0847 p-ISSN : 2320-0936
Volume-7, Issue-7, pp-64-76
www.ajer.org
Research Paper Open Access

# Mapping 3D Geological Structures and Predicting the Kinematics of the Pitwalls Using Photogrammetric Techniques: A Case Study

Baffoe[1], P. E., Boah[1], F. N. And Afam[2], M.
[1](Department of Geomatic Engineering, University of Mines and Technology, Ghana)
[2](Department Geological Engineering, University of Mines and Technology, Ghana)
Corresponding Author: Baffoe1, P. E., Boah

***ABSTRACT:*** *Traditional method of Mapping geological structures in the mine is usually inaccurate, time consuming and very risky, especially in highly unstable areas. The introduction of 3D structural mapping and pit wall monitoring at Perseus Mining Ghana Limited (PMGL), Ayanfuri has boosted safety and higher accuracy mapping in the mine. A suitable approach is the use of the photogrammetric mapping method. The geological structures of the pit walls were captured using Nikon D7000 camera and processed using SiroVision Version 5.1.11.0 software; and the kinematics analysis was done using Dips Version 5.103 software. In all three individual mosaics were created using stereo models of the faces forming a composite image. The structural mapping was performed using Siro Joint, a component of SiroVision; a total of 50 joints were mapped on the photographs. The orientation of the Dip and Dip directions were determined by plotting the mapped structures in Stereonet. This also helped to determine the areas of low to high concentrations using the Frictional Angle, Pit Slope, Daylight Envelope and the Critical Point. The strength of the intact rock was 54 MPa and the Rockmass Rating (RMR) was 57 which helped to define the class and the description within which the rock was found. The cohesion of the rock mass lies between 200-300 Pa and the frictional angle between 25-30 degrees. SET 1 and 2 were kinematically stable but SET 3 was unstable and hence failure is eminent on that plane.*
***KEYWORDS –*** *Dip, Rocks, Sirovision, Steronet, Mapping*

---

Date of Submission: 28-06-2018 Date of acceptance: 13-07-2018

---

## I. INTRODUCTION

Generally, rock mass structural mapping as well as kinematic analysis is made to monitor and understand the behaviour of the rock mass in-situ. This normally helps geotechnical engineers to put measures in place to protect the workers and machinery in the pit from any eventual disaster.

Traditionally, geologists would stand in the open pit or underground mining face to map the rock structures which are visible onto a piece of paper. They would afterward collate the many bits of information on paper and attempt to analyse the structures of the visible rocks; the process could be time consuming, dangerous and inefficient. One of the problems associated with 2D structural mapping is that, there is bias in mapping structures which run perpendicular to the line of sight. It is also very risky and more dangerous to stand under the pit walls to map the geological structures; especially the freshly-blasted face and potentially unstable pit wall. The stability of the pit wall cannot be monitored by normal visual inspection.

A review of literature indicates that, the traditional method takes time both in acquiring and processing the data (Tetteh, 2014). In this method, fieldwork is dangerous, the possibility of rock fall is high and missing potential areas could exist (Poropat, 2014). Due to the risky, biasness and time consuming nature, the traditional method is problematic (Hoek and Bray, 1994). The advent of photogrammetric method of rock structural mapping is a promising technique to curb the potentially hazardous nature of traditional mapping in open pit mining. This method applies sound geotechnical engineering practices, assisting mine design and general operating procedures. This method allows safe and economic mining of any ore within any rock mass and also assists mining operators in achieving their set goals of the mine development. This is done using current geotechnical knowledge, methodology, software and hardware appropriate to the situation (Poropat, 2014).

The behaviour of rock masses is a very important factor in the safety of mining and civil engineering projects. Rock falls are causes of major hazards in the mines and can have fatal consequences. Therefore being able to map the structures of a rock mass is crucial to understanding its potential behaviour. This understanding

can impact positively on safety and efficiency mining or civil engineering projects thereby making geological mapping an important exercise (Hoek and Bray, 1994).

Mapping of the structure of a rock mass may be tedious if pit development plans, graph papers as well as series of strip maps are unavailable. It is unsafe to stand under freshly blasted inaccessible high walls and map unto a paper (Tetteh, 2014). Returning to the office, the geologist would collate the many bits of paper and attempt to analyse the structures which are visible. However, the mining and construction industries require a fast, reliable system of predicting and mapping of rock mass structure. Hence utilizing digital mapping may be a very useful.

The digital mapping of geological structure of rock mass provides the geologist and geotechnical a better understanding of the ore bodies and extension potentials. These tools help them become more proactive by providing a complete view of data required to make decisions to mitigate risk and improve planning. This research work uses modern photo techniques to map geological structures and analyse the rock mass in–situ.

## II. STUDY AREA

The study area comprises two mining leases, the Ayanfuri mining Lease; and the Nanankaw Mining Lease.

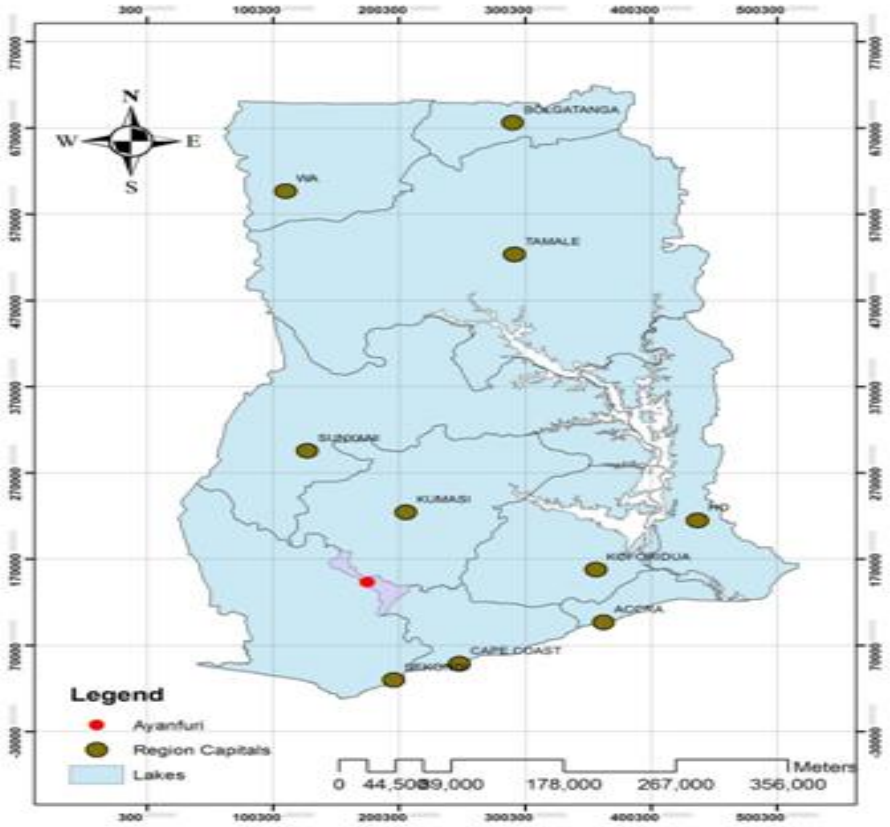


.

**Fig. 1 Location of the Study Area**

These concessions are approximately 49.20 km$^2$ and 43.93 km² respectively, with prospecting area at Dadieso which covers an area of 29.33 km² and that brings together a total land area 122.46 km². The mine concessions are located in the Central Region of Southern Ghana, on the eastern flanks of the highly prospective Ashanti Belt. The areas are located between 1°50'00" west and 2°00'00'' west and 5°48'49'' north and 6°00'00" north. The Project is approximately 57 km to the SW of the municipality of Obuasi and 195 km WNW of the capital Accra ( see Fig. 1) in Ghana, West Africa (Antwi, 2014).

2.1 Geological Settings

The area lies within the Precambrian Guinean Shield of West Africa. The geological formation hosts one of the most important auriferous rocks of metamorphosed and folded Birimian Supergroup (Kesse, 1985). The belt is dominated by a northeast-southwest trending structural feature which extends over 200 km along strike. This structure is closely aligned with a faulted contact zone between the major lithological units: the metasedimentary and metavolcanic and some felsic to mafic intrusive. The metasedimentary sequence is described by Milesi *et al*, (1989) as consisting of very thick beds of argillites and impure arenaceous and

tufaceous sediments called schist, phyllites, greywakes, tuffs and slates. The metavolcanic sequence comprises greenstones of metamorphosed basic lavas and intrusives with complementary felsic lavas and pyroclastic rocks. Manganiferous phyllites associated with hornstone and cherty beds are present in smaller quantities in upper horizons of the greenstones.

Generally, the most common structure at the mine is bedding ($S_o$). It is visible due to the grain size and colour variation, containing well preserved sedimentary structure, Bedding-cleavage intersections are uncommon. $S_o/S_1$ lineations plunge moderately northeast, while $S_o/S_2$ intersections have more diverse orientation. Five structural deformational events have been observed according to recent studies by (Gyapong, 2000). They include:

- $D_1$-Event: Bedding parallel to shearing are non-uniformly distributed. More competent greywacke and volcanics remained unsheared.
- $D_2$-Event: A fold thrust event, produced by moderate to steep dipping linear structures with a NE strike within the Birimian and Tarkwaian sequence.
- $D_3$-Event: This event caused the development of NE trending gentle folds with shallowly NW dipping axial planes. The event was local in nature and appeared to have very little influence on gold distribution.
- $D_4$-Event: Developed a NNE to E tending fold which produced left-stepping flexures in bedding and earlier structures. These left-stepping structures are considered as the principal loci for gold lodes.
- $D_5$-event: Principal Gold Event–induced a few meters to hundreds of meters of largely sinitral (left lateral) reactivation of the NE trending $D_2$ fault zones. This event is considered as the principal source of gold mineralisation of the Birimian systems.

## III. MATERIALS AND METHODS USED

The materials and methods employed in this paper are discussed in the following sections.

### 3.1 Materials Used

An off-the-shelf single-lens reflex (SLR) digital camera, Nikon D7000, with the lens of focal length 60 mm was used; it mounted on a tripod before taking the photographs. The resolution can be achieved at a range between up to 2 000 meters (see Fig. 2).

**Fig. 2 Nikon D7000 Camera**

In addition, Schmidt Hammer was used in measuring the strength of the rock. In measuring the strength, there was the need to measure both the perpendicular and the horizontal strengths and the average taken as shown in Fig. 3.


**Fig. 3 Schmidt Hammer**

In order to georeference the mosaic of 3D photographic images of the rocks, a minimum of three (3) triangulated survey control points are required. These known control points can be any combination of surveyed camera positions (a camera on a tripod) or ground control points marked on to the actual rock surface. These points were surveyed using GPS receivers. There was a base station and rover receivers such as from Trimble incorporation with Geotaggers. These systems write GPS metadata onto the photographs as they are taken. The major advantages of this system are:

- The GPS data contained on the photographs file metadata.
- Photographs can be rapidly taken hand-held, with no tripods necessary.
- There is no requirement for external survey support.

There is no requirement to access the rock face to place control points, saving time and improving safety

### 3.2 Methods Used

The data was collected on the AG stage 3-East pit wall of Perseus Mining Ghana Limited. This was done using the camera to take photographs to map the various geological structures and also monitor its rate of movement to be able to analyse them.

#### 3.2.1 Planning the Mapping

The mapping task is first evaluated to ascertain the size of features to be mapped and the accuracy required; this helped to determine the lens to be used with a given camera and the geometry of the camera Ground Base. The camera positions were strategically selected such that the separation between the positions is approximately one sixth of the distance to the face being mapped. In order for the mosaic of the 3D images to be accurately constructed, the camera positions were chosen so as to provide sufficient overlap to form the stereo model of the 3D images produced to build a mosaic with good coverage.

#### 3.2.2 Field Procedures

In order to create accurately scaled 3D photographic images, three basic rules are applied as stipulated in photogrammetric ground measurements rules:

- The left and the right photographs of the same rock face must be taken to produce a stereopair;
- The left and right photographs must have a baseline (distance between camera positions) at very roughly a ratio of 1:7 to the distance to the rock face; and
- In order to mosaic 3D images together, adjacent stereopairs must overlap by around 30%.

#### 3.2.3 Data Collection

To achieve the purpose of this task, primary data was obtained from the AG stage 3- East pit wall in the mine. The Dip and Dip Directions, the persistence, orientations as well as the displacement were determined through stereo photogrammetry. The data obtained were later transformed into the national grid where the Nothings, Eastings and Heights of each point on the wall were collected. Also, vital information was obtained from the Geotechnical Section of the mine with regards to the geology of the rock, the rock type, angle of repose, the strike and dip of the rock, the effect of the water table on the rock and some geological factors. These parameters aided in the investigation of the principal causes of displacement and how it influences failure of the pit wall.

#### 3.2.4 Image Acquisition

The camera was set up on the tripod and aligned so that the chosen face is on or near the vertical centre line of the image. It was ensured that the camera and the tripod were levelled. The camera was then focused and the exposure station was constructed into the correct position. Relative Orientation facilities were used to determine camera orientation. Also it was ensured that there was enough overlap in the two images to determine the camera orientation. The location of the camera was marked using a spray marker on the ground directly beneath the camera. It was ensured that the mark was vertical below the appropriate point of the camera – this is usually the intersection of the central axis of the lens and the mounting flange for the lens.

The instrument height of the camera on both the left control (LC) and the right control (RC) were recorded to be 1.5 m and 1.52 m respectively above the mark using the height from the mark to the position used for defining camera position (above) and was added to the reduced level (RL) of the pit.

The Second and third images were captured by repeating the procedure to the first pair remembering to ensure that the camera is levelled to start; the camera is then focused and that the exposure is ‘good’; the camera position is marked with an appropriate reference on the ground and record the camera height above the mark.

A distance, ‘**S**’ of 48m was measured from the pit floor to the face of the pit wall using a laser. This was done perpendicular to the control point on the wall so that the left and right camera positions could be established. The Baseline distance ‘**B’** (m) is given by;

**B** = $\frac{5}{7}$ , **B** = $\frac{48}{7}$ = **6.8 m ,** since there are two camera positions, **B** is divided by two in order to get an equal distance from the line of perpendicular to the left and right positions. Hence, $\frac{6.8}{2}$, was used to determine an equal distance of 3.4 m from the line of perpendicular to the left and right positions respectively. The Figure 4 below shows how the images were taken.

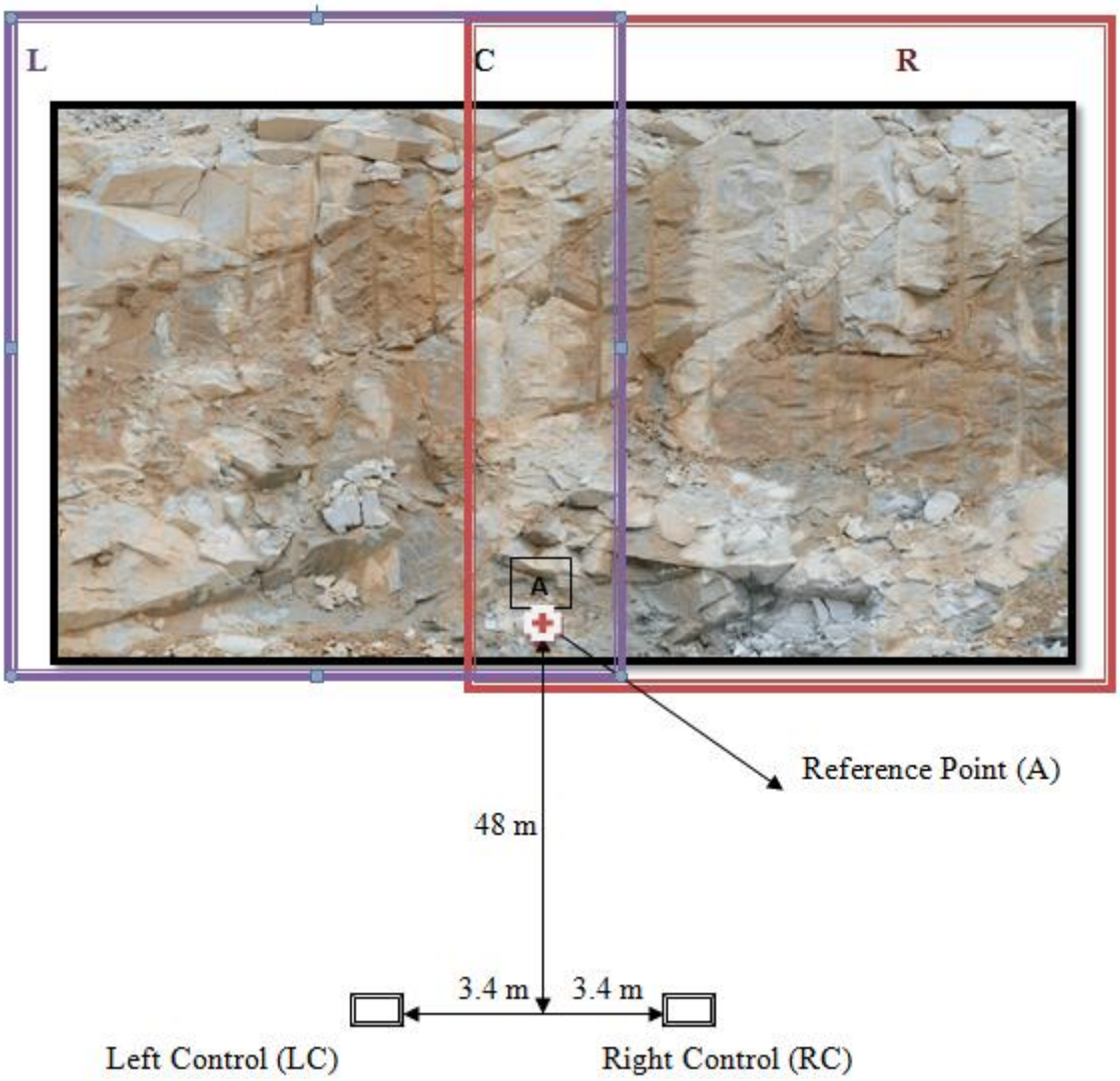


**Fig.~~ure~~ 4 Method of obtaining Photographs for Sirovision**

### 3.3 Images Correction

The captured data is then downloaded from the camera in a raw format. They were then converted into TIFF images. For many cameras these can be 8 bit or 16 bit but for most applications 8 bit images are sufficient. Archive the raw images if required. The images are processed in order to correct for lens distortion.

These image corrections were done by applying image support and parameter of the lens that was used, selected from the menu of the software. The software then checked camera parameters such as camera model and lens focal length. It was ensured that these were chosen when the processes started. Once all the images have been corrected for lens distortion, the captured data is imported into the processing software called Sirovision as photographic images.

### 3.4 Georeferencing

To use the data effectively in the set of software packages selected for the work, the captured and corrected images were georeferenced in Sirovision software. The process provided a way whereby survey data,

metadata, and attributes were integrated with the images. To fully complete the georeferencing process, the mosaic of 3D images, a minimum of 3 triangulated control points were required. These known points can be any combination of surveyed camera positions (a camera on a tripod) or ground control points marked on to the actual rock surface. These points were surveyed using RTK GPS mode method, using base stations as well as rover receivers.

## IV. RESULTS AND DISCUSSIONS

### 4.1 Images Taken

The images are taken in series, left, central and right. The first central image was taken containing the control point when stood on the left base station (FCL) and this is as seen in Fig. 5. Also, the image taken from the first central containing the control point when stood on the right base station (FCR) as in Fig. 6. The second left image containing the control point was taken when the camera was set on the left base station (SLL) as seen in Fig. 7. The third right image containing the control point was also taken when the camera was set on the left base station (TRL) as shown in Fig. 8**.** The second left image containing the control point was also taken when the camera was set on the right base station (SLR) as shown in Fig. 9**.** Then the **t**hird right image containing the control point was taken when the camera was set on the right control (TRR) as shown in Fig. 10.

**Fig. 5 First Central Image Containing the Control Point when Stood on the Left Control (FCL)**

**Fig. 6 Second Left Image Containing the Control Point when Stood on the Left Control (SLL)**

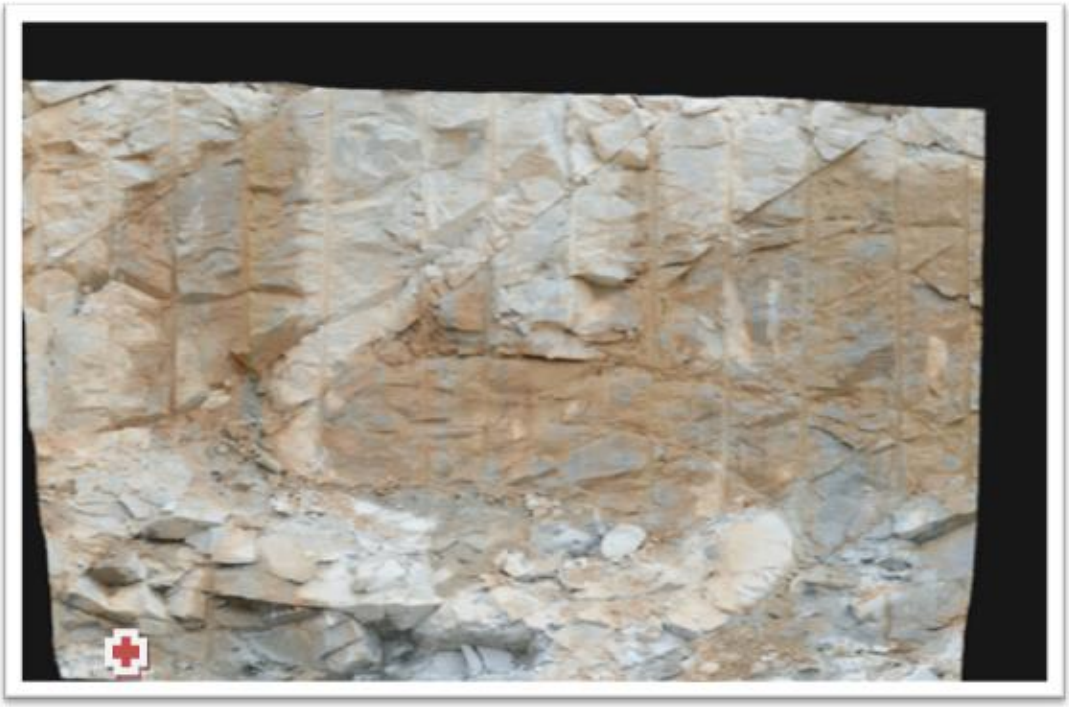

**Fig. 7 Third Right Image Containing the Control Point when Stood on the Left Control (TRL)**

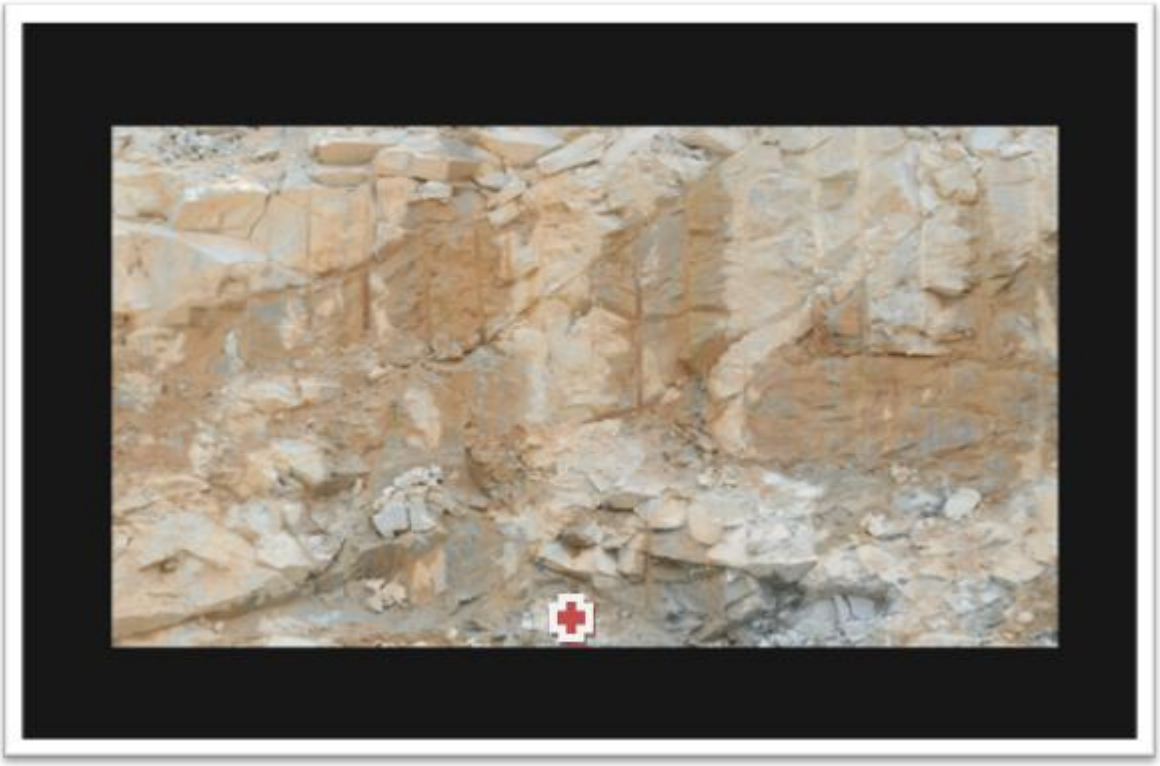

**Fig. 8 First Central Image Containing The Control Point when Stood on the Right Control (FCR)**

**Fig. 9 Second Left Image Containing the Control Point when Stood on the Right Control (SLR)**

**Fig. 10 Third Right Image Containing the Control Point when Stood on the Right Control (TRR)**

**4.2 Mosaic**

Mosaic is the pattern of putting pieces of pictures together to form one image. From Fig. 5, 6, 7, 8, 9 and 10, a mosaic was formed by combining FCL and FCR images, SLL and SLR images and TRL together with TRR images. In all, three (3) individual mosaics were formed. The three mosaics were combined to form a composite image as seen in Figure 11.

American Journal of Engineering Research (AJER)
e-ISSN: 2320-0847 p-ISSN : 2320-0936
Volume-7, Issue-7, pp-64-76
www.ajer.org
Research Paper Open Access

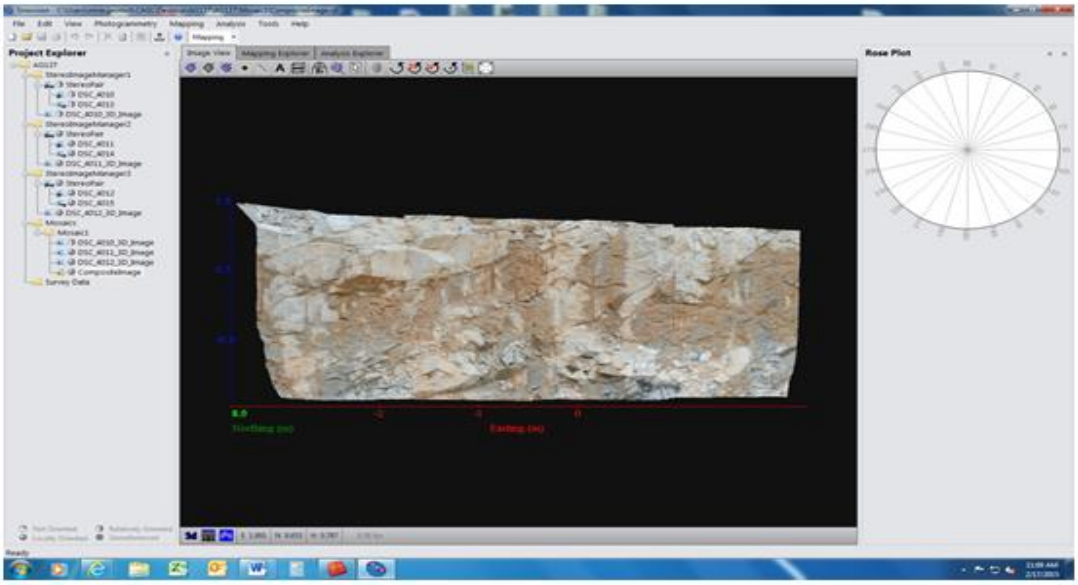

**Fig. 11 Composite Image**

### 4.3 Structural Mapping

Structural mapping was performed on the composite image using SiroJoint, a component of Sirovision software. A total of about 50 joints structures were mapped directly on the photograph. The figures below shows the siroJoint mapped joints of the rock face. The arrows show the direction of the geological structures thus dip/dip directions of the mapped structures, letters A and B show the beginning and the ending of the mapped joints structure respectively as shown in Fig. 12 and 13.

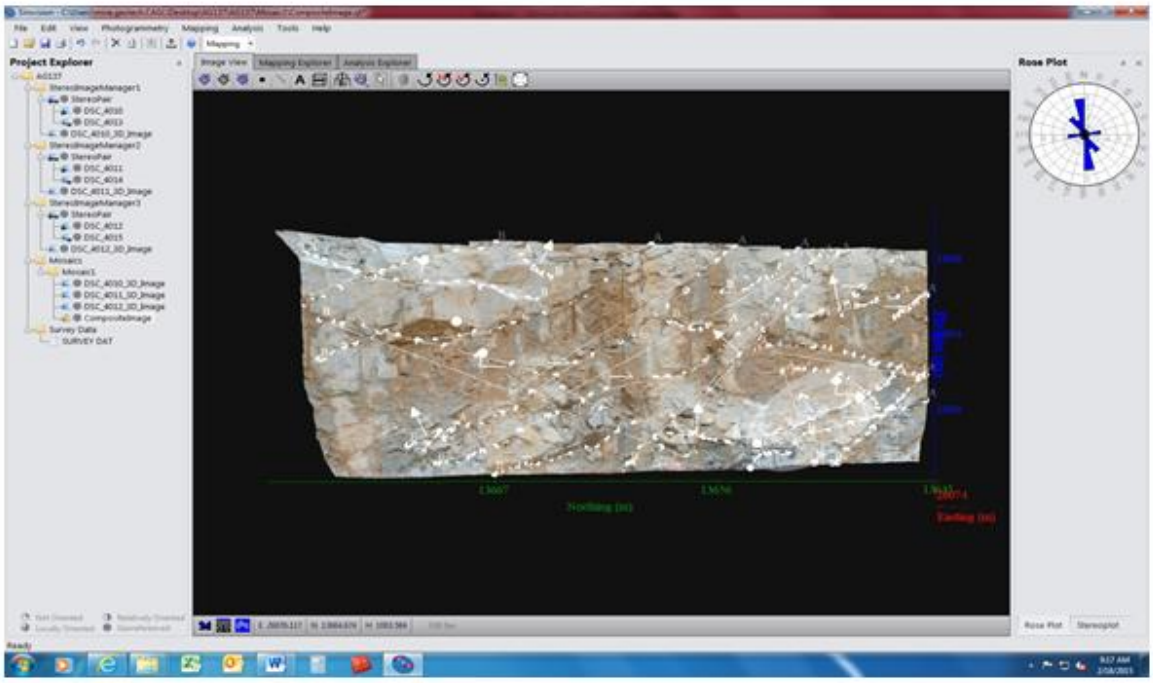

**Fig. 12 Mapped Structures of the Rock Face using SiroJoint**

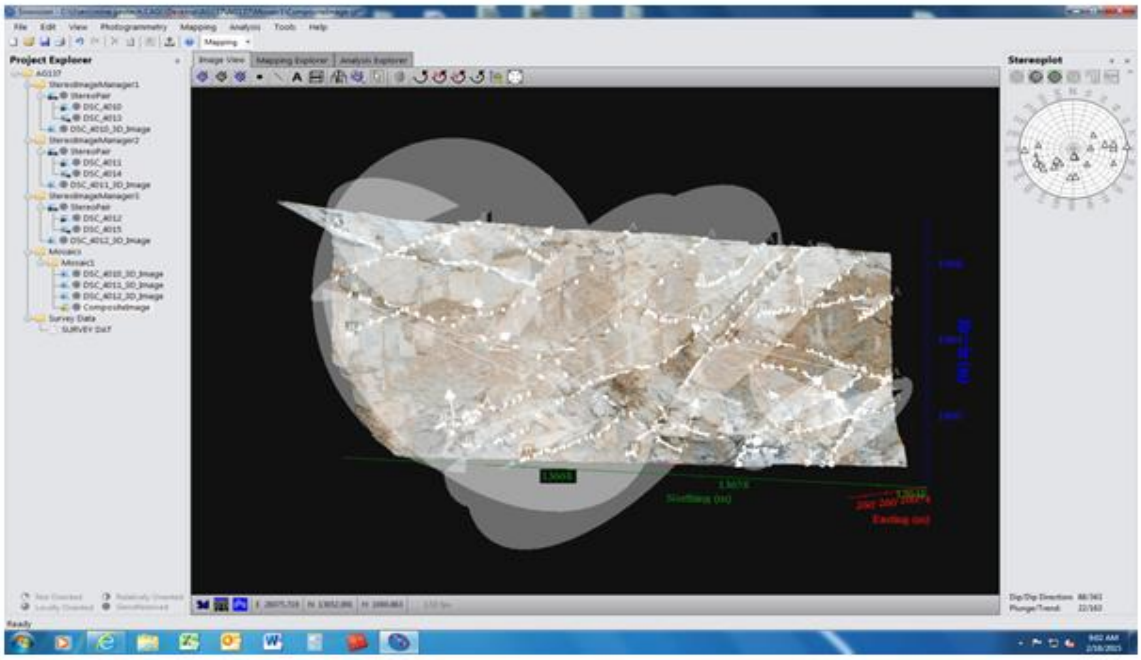

**Fig. 13 Planes of the Mapped Surfaces Generated**

After mapping the geological structures, the various dip/dip direction, the controls (Easting, Northing and the Reduced Levels), and the type of structures mapped, orientations as well as the persistence were generated. The Fig. 14 shows the information on the composite image in the database structure.

Dips - [AG1.dip*]

File Edit Setup View Select Sets Tools Window Help

| ID | Dip | Dip Direction | EASTING | NORTHING | RL | LENGTH | NAME | RELIABILITY | RMS METRES | SIGMA DEGS | MODEL NAME |
|---|---|---|---|---|---|---|---|---|---|---|---|
| 1 | 58 | 64 | 26074.442 | 13663.884 | 998.072 | 6.666 | JN | N/R | 0.011 | 17.957 | CompositeImage |
| 2 | 51 | 50 | 26076.204 | 13654.361 | 1005.517 | 10.231 | JN | N/A | 0.072 | 35.680 | CompositeImage |
| 3 | 77 | 81 | 26075.746 | 13673.375 | 1007.355 | 6.666 | JN | N/A | 0.071 | 37.978 | CompositeImage |
| 4 | 64 | 78 | 26075.702 | 13674.375 | 1003.748 | 3.985 | JN | N/A | 0.033 | 22.088 | CompositeImage |
| 5 | 81 | 79 | 26075.714 | 13663.828 | 1003.371 | 22.504 | JN | N/A | 0.164 | 24.394 | CompositeImage |
| 6 | 48 | 8 | 26076.053 | 13652.809 | 1005.664 | 8.948 | JN | N/A | 0.049 | 26.111 | CompositeImage |
| 7 | 40 | 356 | 26074.227 | 13648.191 | 999.630 | 7.385 | JN | N/A | 0.106 | 27.150 | CompositeImage |
| 8 | 86 | 285 | 26075.224 | 13647.464 | 1007.491 | 3.804 | JN | N/A | 0.072 | 46.477 | CompositeImage |
| 9 | 79 | 278 | 26075.834 | 13650.960 | 1002.095 | 6.437 | JN | N/A | 0.060 | 15.511 | CompositeImage |
| 10 | 44 | 342 | 26075.485 | 13657.982 | 1000.005 | 7.100 | JN | N/A | 0.096 | 25.815 | CompositeImage |
| 11 | 62 | 277 | 26074.663 | 13652.607 | 999.884 | 13.293 | JN | N/A | 0.269 | 44.537 | CompositeImage |
| 12 | 85 | 251 | 26075.833 | 13651.640 | 1007.743 | 1.589 | JN | N/A | 0.012 | 12.208 | CompositeImage |
| 13 | 73 | 82 | 26076.332 | 13654.287 | 1005.180 | 6.218 | JN | N/A | 0.045 | 16.923 | CompositeImage |
| 14 | 34 | 31 | 26076.410 | 13660.655 | 1007.647 | 5.255 | JN | N/A | 0.064 | 23.330 | CompositeImage |
| 15 | 64 | 95 | 26076.482 | 13657.579 | 1005.033 | 3.176 | JN | N/A | 0.054 | 18.902 | CompositeImage |
| 16 | 90 | 251 | 26076.365 | 13659.216 | 1003.399 | 2.012 | JN | N/A | 0.023 | 70.137 | CompositeImage |
| 17 | 76 | 84 | 26076.209 | 13667.255 | 1005.005 | 9.018 | JN | N/A | 0.115 | 58.088 | CompositeImage |
| 18 | 77 | 280 | 26075.645 | 13649.609 | 1003.412 | 2.237 | JN | N/A | 0.025 | 68.314 | CompositeImage |
| 19 | 51 | 249 | 26076.245 | 13664.269 | 1007.657 | 2.367 | JN | N/A | 0.011 | 11.770 | CompositeImage |
| 20 | 68 | 83 | 26076.445 | 13665.872 | 1007.464 | 2.229 | JN | N/A | 0.029 | 18.351 | CompositeImage |
| 21 | 32 | 261 | 26076.034 | 13670.115 | 1007.356 | 5.758 | JN | N/A | 0.040 | 13.380 | CompositeImage |
| 22 | 57 | 267 | 26075.637 | 13674.780 | 1001.308 | 3.025 | JN | N/A | 0.073 | 72.250 | CompositeImage |
| 23 | 84 | 91 | 26075.604 | 13672.818 | 1001.927 | 6.582 | JN | N/A | 0.086 | 28.049 | CompositeImage |
| 24 | 35 | 77 | 26076.587 | 13662.201 | 1008.528 | 4.017 | JN | N/A | 0.067 | 30.635 | CompositeImage |
| 25 | 88 | 241 | 26076.432 | 13663.019 | 1007.175 | 1.853 | JN | N/A | 0.028 | 49.285 | CompositeImage |
| 26 | 74 | 87 | 26074.599 | 13646.193 | 1000.458 | 1.174 | JN | N/A | 0.036 | 34.202 | CompositeImage |
| 27 | 83 | 297 | 26075.605 | 13649.472 | 1006.020 | 1.323 | JN | N/A | 0.021 | 54.640 | CompositeImage |
| 28 | 64 | 283 | 26075.212 | 13647.629 | 1006.511 | 3.268 | JN | N/A | 0.016 | 67.717 | CompositeImage |
| 29 | 81 | 279 | 26075.101 | 13647.278 | 1005.648 | 3.682 | JN | N/A | 0.032 | 24.630 | CompositeImage |
| 30 | 54 | 96 | 26074.850 | 13658.264 | 998.494 | 1.608 | JN | N/A | 0.015 | 18.578 | CompositeImage |
| 31 | 40 | 100 | 26074.849 | 13656.591 | 998.370 | 2.203 | JN | N/A | 0.034 | 19.459 | CompositeImage |
| 32 | 87 | 283 | 26074.730 | 13656.979 | 997.644 | 1.990 | JN | N/A | 0.073 | 69.219 | CompositeImage |
| 33 | 40 | 102 | 26074.138 | 13652.541 | 998.170 | 5.470 | JN | N/A | 0.118 | 18.289 | CompositeImage |
| 34 | 41 | 210 | 26074.691 | 13664.852 | 999.124 | 1.016 | JN | N/A | 0.029 | 72.226 | CompositeImage |
| 35 | 88 | 256 | 26074.549 | 13663.534 | 998.697 | 1.899 | JN | N/A | 0.081 | 52.493 | CompositeImage |
| 36 | 70 | 149 | 26074.633 | 13663.742 | 998.976 | 1.412 | JN | N/A | 0.012 | 64.831 | CompositeImage |

AG1.dip* Dips1

For Help, press F1

**Fig. 14 Data from 3D Models using Dips software in a Structured Database**

### 4.4 Kinematics Analysis

Kinematic analysis was done as a means of monitoring the stability of rock mass in-situ that have geological structures posing risk in them and could fail and cause damage on workers or the machinery. In kinematic analysis, Rock Mass Rating and Daylight Envelope are major factors that contribute to the rock mass analysis. Daylight Envelopes are used primarily in slope stability analysis work. It is kinematically feasible for any poles that plot within a Daylight Envelope to slide. To determine the stability of such poles, one must also consider the frictional strength, also known as the friction angle, thus the force of attraction between the rock mass in situ of the planes. Rockmass Rating system helps to determine the integrity of the rockmass. This system was established by Bieniawski (1976) and was updated in 1989. Both versions were used to achieve these results as tabulated below. The slope of the pit has a dip/direction of 53/270. This means that, any structure which daylight the slope angle and has frictional strength greater than that of the rock mass structure, sliding is kinematically possible for these planes hence is likely to fail.

### 4.5 Geological Structure and Rockmass Strength

Rock failure occurs when the driving forces acting on a given body of material exceed the resisting forces within that body of material. In a freshly excavated slope, the force resisting failure can be attributed to the shear strength of the rock mass and the mobilised fictional resistance. The driving force is primarily dependent on the unit weight of the rock mass, the geometry of the slope and the potential modes of failure. In soft rock, failure can propagate through the intact rock or along geological structure. In hard rock the path of minimum shear strength is predominantly along rock mass geological structure. It follows, therefore, that mine operators must identify the relevant modes of failure (the sources and magnitudes of the potential driving forces), and also determine and quantify the shear strength and other forms of resisting forces pertinent to that rock mass and mode of failure.

**Table 1 Rockmass Rating for the Rocks (after Bieniawski, 1989)**

| | **PARAMETER** | **RANGE OF VALUES** |
|---|---|---|
| 1 | Strength of intact rock material (54 MPa) | 50-100 MPa |
| | Rating | 7 |
| 2 | Space of discontinuity (1.19 m) | 0.6-2.0 m |
| | Rating | 15 |
| 3 | Condition of discontinuity | Slightly rough surfaces, Separation less than 1 mm. Slightly weathered walls |
| | Rating | 25 |
| 4 | Ground water | Damp |
| | Rating | 10 |
| | **Total Rating Value** | **57** |
| **Rock Mass Classes Determined From Total Rating** | | |
| Rating | | 41-60 |
| Class number | | III |
| Description | | Fair rock |
| **Meaning of Rock Classes** | | |
| Class number | | III |
| Cohesion of rock mass (KPa) | | 200-300 |
| Friction angle of rock mass (Degree) | | 25-35 |

From Table 1, it can be seen that the friction angle of the rock mass (degrees) lies between 25 and 35 degrees. This means that any value from 25º to 35º can be used. With this, 35º was used as the frictional strength of the rock mass and was plotted as seen in the figures below. The slope of the pit has a dip/dip direction of 53/270 respectively. This was also plotted in the Stereonet or Dips as seen in Fig. 15 and 16.

.

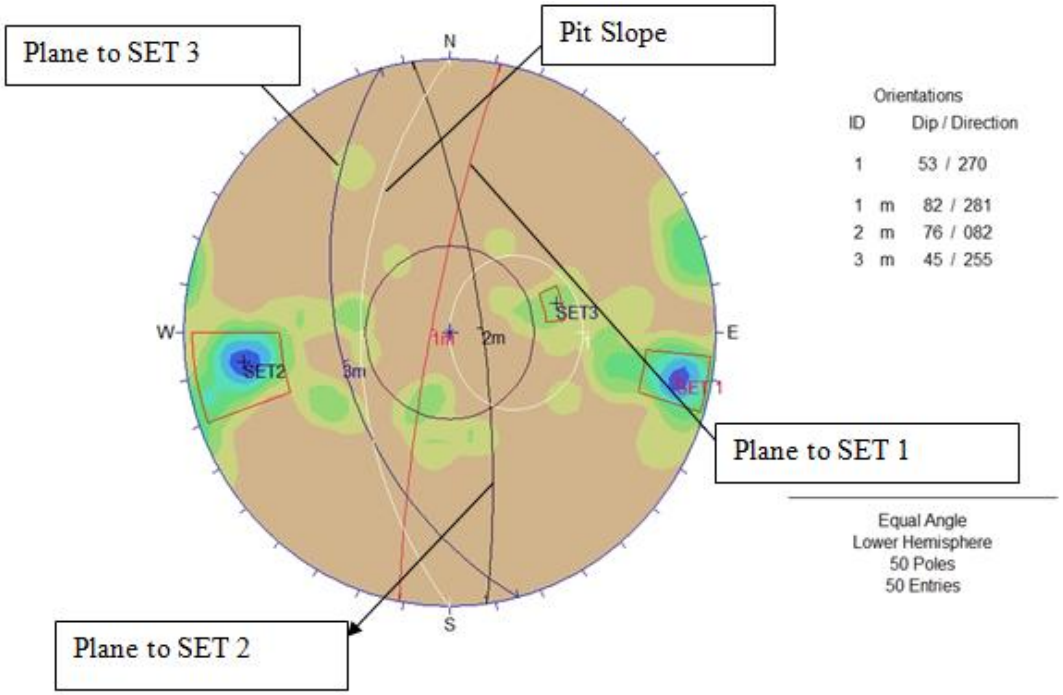


**Fig. 15 Dip/Dip Directions of Mapped Structures Plotted in Stereonet Showing the Orientations of the three (3) Sets**

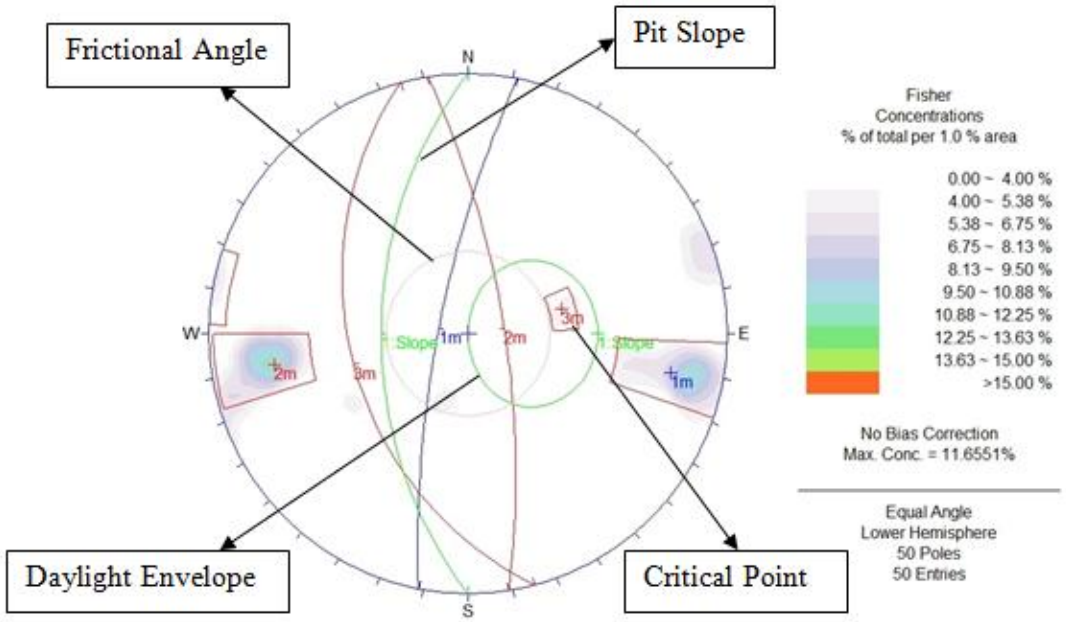


**Fig. 16 Dip/Dip Directions of Mapped Structures Plotted in Stereonet Showing the Concentrations from Low to High Concentrated Area**

**4.6 Discussion**

From the table, it can be seen that, the strength of intact rock material has a value of 54 MPa, which falls in the rage of 50-100Mpa, hence giving a rating of 7. The space of discontinuity is 1.19 m and lies between 0.6-2.0 m, giving a rating value of 15, condition of discontinuity of the face is slightly rough surfaces, separation less than1 mm and also the walls are slightly weathered. This has a rating of 25. The ground water (general water condition) is damp, giving a rating value of 10. The various rating values were put together giving a total

rating value of 57. This rated value was used to define the class and the description within which the rock is found. It has been shown that, the rocks have a class of III with the description being a fair rock. Cohesion of rock mass (kPa) lies between 200-300 and the frictional angle of rock mass (Degree), is between 25-35 degrees.

In all, there are three (3) joint sets. Figure 15 shows the orientations of the three sets whilst Figure 16 depicts the fisher concentrations in percentage (%) of total per 1 % area, with a maximum concentration of 11.6551%. SET 1, SET 2 and SET 3 with their orientations or planes are shown in Figure 15. The area within the Daylight envelope, from Figure 16 contains the poles to planes which have dip vectors outside the slope (i.e. sliding is kinematically possible for these planes). The daylight envelope represents all planes which can theoretically daylight from a given slope. In practice, planes which have a similar dip direction to the slope plane are more likely to fail.

SETS 1 and 2 though, are high in concentration of the joint structures but are kinematically stable. This is because, they are neither found within the friction circle nor the daylight envelope. Thus, for poles that plot inside the daylight envelope, but outside the friction circle, sliding is possible, hence SET 3. This is found inside the daylight envelope, but outside the friction circle. This means that, failure is likely to occur and the type of failure that can occur is planer failure. This is because, the failure will occur along the plane of the pit.

## V. CONCLUSION

Geological structural mapping and monitoring using the traditional method is very tedious, time consuming and dangerous. All these shortcomings associated with traditional geological mapping method make the Digital 3D mapping relatively safer and more convenient, effective and efficient.

Sirovision software package has been used to map the 3D images of geological structures to determine the potential for toppling, wedge and planar failures through kinematic analysis. The designed size, shape and orientation of open pit excavations relative to the geological structure need to be recognised as a major factor controlling the number, size and shape of potentially unstable blocks that may form within the pit walls.

The structural mapping was performed using SiroJoint, a component of Sirovision; a total of 50 joints were mapped on the photographs. The orientation of the Dip and Dip directions were determined by plotting the mapped structures in Stereonet. This also helped to determine the areas of low to high concentrations using the Frictional Angle, Pit Slope, Daylight Envelope and the Critical Point. The strength of the intact rock was 54 MPa and it falls in the range of 50-100 MPa hence rate 7. The space of discontinuity was 1.9 m which lies between 0.6-2.0 and was given a rating the value of 15 condition of discontinuity of the face thus slightly weathered and rated 25. The various rating values were put together giving the total rating value of 57 which helped to define the class and the description within which the rock was found. The cohesion of the rock mass lies between 200-300 KPa and the frictional angle between 25-30 degrees. SET 1 and 2 were kinematically stable but SET 3 is unstable therefore sliding and hence failure is possible.

It is recommended that, all mining and civil engineering industries should adopt this modern method of mapping which is fast, safe and more efficient method for mapping and monitoring. It is also recommended that, the mosaic of the whole mine should be generated for effective mine design and planning.

## REFERENCES


[1]. M. J. Little, Understanding and managing kinematic failure on the west wall at Sandsloot open pit, *Proc. 18th Conf. of the Young Geotechnical Engineers*, Swadini. 1985, 203-219.
[2]. G. M. Tetteh, *Mining Geology and Laws*, doctoral diss., University of Mines and Technology, UMaT, Tarkwa, Ghana, 2014.
[3]. E. Hoek and J. W. Bray, *Rock slope engineering* (Chapman & Hall, USA, 1994).
[4]. Bieniawski, E. (1976), *Rock Mass Rating*, www.globalmining.com. Accessed: February 18, 2015.
[5]. M. Antwi, *Pit Wall Monitoring at Perseus Mining Ghana Limited, Ayanfuri: A Case Study*, doctoral diss., University of Mines and Technology, Tarkwa, 2014.
[6]. H. Romana, *Geological standard index* (Bulletin of Engineering Geology and the Environment, USA, 1989).
[7]. M. Jami and P. E. Girard, *Assessing and monitoring open pit mine high walls* (National Institute for Occupational Safety and Health, Spokane Research Laboratory, 315 E. Montgomery Ave., Spokane, WA 99207, 2001).
[8]. W. B. John and J. L. *Richard, basic geological mapping* (John Wiley and sons Ltd, West Sussex, England, 4th ed., 2015)
[9]. G. V. Poropat, Automated Structure Mapping of Rock Faces, Proc. of International Symposium on Stability of Rock Slopes in Open Pit Mining and Civil Engineering, South Africa, 2001).


.

Baffoe1, P. E., Boah"Mapping 3D Geological Structures and Predicting the Kinematics of the Pitwalls Using Photogrammetric Techniques: A Case Study."American Journal of Engineering Research (AJER), vol. 7, no. 07, 2018, pp. 64-76.